

This is the post-print version of the following article: Rejc, L; Gómez-Vallejo, V; Rios, X; Cossío, U; Baz, Z; Mujica, E; Gião, T; Cotrina, EY; Jiménez-Barbero, J; Quintana, J; Arsequell, G; Cardoso, I; Llop, J., [Oral Treatment with Iododiflunisal Delays Hippocampal Amyloid- \$\beta\$ Formation in a Transgenic Mouse Model of Alzheimer's Disease: A Longitudinal in vivo Molecular Imaging Study](#), *Journal of Alzheimer's Disease*, 2020

“The final publication is available at IOS Press through <http://doi.org/10.3233/JAD-200570>”.

This article may be used for non-commercial purposes in accordance with IOS Press Terms and Conditions for Self-Archiving.

TITLE

Oral treatment with iododiflunisal delays hippocampal amyloid beta formation in a transgenic mouse model of Alzheimer disease: a longitudinal *in vivo* molecular imaging study.

AUTHORS

Luka Rejc^{a,*}, Vanessa Gómez-Vallejo,^b Xabier Rios,^b Unai Cossio,^b Zuriñe Baz,^b Edurne Mujica,^c Tiago Gião,^{d,e} Ellen Y. Cotrina,^f Jesús Jiménez-Barbero,^{g,h,i} Jordi Quintana,^{j,k} Gemma Arsequell,^f Isabel Cardoso,^{d,e,**} Jordi Llop^{b,l,†}

AFFILIATIONS

^a University of Ljubljana, Faculty of Chemistry and Chemical Technology, Večna pot 113, Ljubljana, Slovenia.

^b CIC biomaGUNE, Basque Research and Technology Alliance (BRTA), 20014 San Sebastian, Guipuzcoa, Spain.

^c Biochemistry and Molecular Biology, EHU-UPV, Leioa, Spain.

^d IBMC - Instituto de Biologia Molecular e Celular, Porto, Portugal.

^e i3S – Instituto de Investigação e Inovação em Saúde, Universidade do Porto, Porto, Portugal.

^f Institut de Química Avançada de Catalunya (I.Q.A.C.-C.S.I.C.), 08034 Barcelona, Spain

^g CIC bioGUNE, Basque Research and Technology Alliance (BRTA), Bizkaia Technology Park, 48160 Derio, Bizkaia, Spain

^h Ikerbasque, Basque Foundation for Science, Maria Diaz de Haro 3, 48013 Bilbao, Spain.

ⁱ Department Organic Chemistry II, Faculty Science & Technology, EHU-UPV, Leioa, Spain.

^j Plataforma Drug Discovery, Parc Científic de Barcelona (PCB), Barcelona, Spain.

^k Current affiliation: Research Programme on Biomedical Informatics, Universitat Pompeu Fabra, Barcelona, Spain

^l Centro de Investigación Biomédica en Red – Enfermedades Respiratorias (CIBERES)

* e-mail: luka.rejc@fkkt.uni-lj.si, ** icardoso@ibmc.up.pt; † jllop@cicbiomagune.es

RUNNING TITLE

Iododiflunisal delays A β formation in AD mice

ABSTRACT

Transthyretin (TTR) is a tetrameric, Amyloid-beta (A β)-binding protein, which reduces A β toxicity both *in vitro* and *in vivo*. The ability of TTR to interact with A β can be enhanced by a series of small molecules that stabilize its tetrameric form. Hence, TTR stabilizers might act as disease-modifying drugs in Alzheimer disease (AD). In this work, we monitored the therapeutic efficacy of two TTR stabilizers, iododiflunisal (IDIF), which acts as small-molecule chaperone (SMC) of the TTR/A β interaction, and the drug tolcapone, which stabilizes tetrameric TTR but does not behave as an SMC, in an animal model of AD using positron emission tomography (PET). Female mice (A β PP^{swe}/PS1A246E/TTR^{+/-}; n=21) were divided into 3 groups (n=7 per group): IDIF-treated, tolcapone-treated and non-treated (control). The oral treatment (100 mg/Kg/day) was started at 5 months of age. Treatment efficacy assessment was based on changes in longitudinal deposition of A β in the hippocampus (HIP) and the cortex (CTX) at ages=5-14 months and determined using PET-[¹⁸F]florbetaben. Immunohistochemical (IHC) analysis was performed at age=14 months. Standard Uptake Values relative to the cerebellum (SUVr) of [¹⁸F]florbetaben in CTX and HIP of non-treated animals progressively increased from age=5 to 11 months and stabilized afterwards. In contrast, [¹⁸F]florbetaben uptake in HIP of IDIF-treated animals remained constant between ages=5 and 11 months and significantly increased at 14 months. In tolcapone-treated group, SUVr progressively increased with time, but at lower rate than in non-treated group. No significant treatment effect was observed in CTX of IDIF- or tolcapone-treated animals. Results from IHC matched the *in vivo* data at age=14 months. Altogether, our work provides encouraging preliminary results on the ability of small-molecule chaperones to ameliorate A β deposition in certain brain regions.

KEYWORDS.

PET, positron emission tomography, Alzheimer disease, disease-modifying drug, transthyretin, small-molecule chaperones, TTR/A β interaction.

MAIN TEXT

1. Introduction

Alzheimer disease (AD) is the most common cause of dementia. It is the fifth leading cause of death globally, with a total of 2.4 million deaths in 2016, and the second leading cause of death among those over the age of 70. Alarmingly, these numbers are increasing and are estimated to reach 50 million dementia patients by 2050, worldwide [1]. Pathophysiologically, AD is characterized by the accumulation of amyloid-beta (A β) aggregates [2], the occurrence of neurofibrillary tangles (NFTs) of hyperphosphorylated tau protein [3], and synaptic dysfunction [4]. In addition, AD progression is accompanied by neuroinflammation [5], structural cerebrovascular alterations and deficits in cerebral glucose uptake and cerebral blood flow responses [6].

Knowledge gained on AD has enabled the development of a variety of mechanism-based therapeutic approaches, which aim at slowing down or stopping the disease progression. Most investigated treatment strategies include: (i) minimizing the amount of A β in the brain by inhibiting A β production, preventing A β aggregation or accelerating A β clearance from the brain; (ii) minimizing aggregation or post-translational modifications of tau protein; and (iii) targeting apolipoprotein E (ApoE) [7]. Other neuroprotective strategies involve the use of neurotrophins and target neuroinflammation or oxidative stress. Nevertheless, despite decades of efforts, there is still no cure for AD. The outcome is especially worrying because over the last decade more than 50 drug candidates successfully passed phase II clinical trials but all failed in

more advanced phases [8-12]. Currently, there are only 132 agents in clinical trials for the treatment of AD [9] compared to more than 3558 drugs employed in cancer trials [13]. The absence of an approved disease-modifying therapy (DMT) calls for an immediate intervention, by feeding new drug candidates into the currently exhausted AD drug development pipeline of phase I clinical trials.

One possibility of alleviating AD pathophysiological stress suggests reducing levels of A β and its toxic species by enabling their transport out of the brain with the help of intrinsic proteins. Research in the past decade revealed that interactions of molecular chaperone proteins with toxic A β species minimize their harmful effects on the central nervous system (CNS) [14-17]. Several intrinsic proteins were shown to be capable of modifying the stability/aggregation, circulation and clearance characteristics of A β peptides [18]. Some examples of these proteins include Gelsolin [19], Apolipoprotein J (clusterin) [20, 21], ApoE [22], and human serum albumin (HSA) [23-25]. In fact, the AMBAR (Alzheimer Management by Albumin Replacement) program, currently in phase III clinical trials, has shown promising results in treatment of moderate AD dementia patients based on the HSA/A β interaction [26].

Another amyloid binding protein that helps transport A β peptides across the blood-brain barrier (BBB) is Transthyretin (TTR) [27-31]. This 55 kDa homotetramer [32] is present in the serum and cerebrospinal fluid (CSF) and is the main A β binding protein in human CSF. Although there are many reported *in vitro* studies of the interaction of TTR with A β [33-36], the molecular mechanisms of TTR neuroprotection have not been fully elucidated. Some researchers suggest that TTR interferes with A β by redirecting oligomeric nuclei into non-amyloid aggregates [37], and very recently, other authors have reported that TTR seems to inhibit both primary and secondary nucleations of A β

peptide aggregation, reducing the toxicity of their oligomers [38]. Furthermore there is still controversy around which TTR species is relevant for A β -related protection (or for the inhibition of A β aggregation or re-directing oligomers into inert species). While some authors showed that, *in vitro*, there is an inverse relation between the strength of the inhibition of A β aggregation and fibril formation and the stability of TTR [33], other results show that the stability of the tetrameric form of TTR plays a pivotal role in amyloidogenic properties of the protein [39], and that unstable TTR complexes bind poorly to A β peptide [40]. Studies on AD patients have shown that TTR has reduced ability to carry its natural stabilizer thyroxine (T₄) in blood plasma [41], and that the folded/monomeric ratio of TTR is decreased in AD patients [42]. At the preclinical level, the presence of resveratrol in AD mice led to the reduction of A β plaque burden and of total A β brain levels [34], and to the deceleration of TTR clearance and restoration of normal concentration levels of TTR in the brain [43] and in plasma [44], possibly due to favored TTR dimer-dimer interaction. All these results suggest a pivotal role of the tetrameric form of TTR in A β -related protection, but the controversy on the topic encourages further research that would give a better insight into the disease mechanism.

In a previous study, our group has shown that the TTR tetramer stabilizer iododiflunisal (IDIF; Figure 1), a iodinated derivative of the non-steroidal anti-inflammatory drug (NSAID) diflunisal, promotes A β clearance from the brain and improves animals' cognitive functions when orally administered to AD transgenic mice (A β PP^{swe}/PS1A246E/TTR^{+/-}) daily for 2 months, starting just before the onset of the disease [45]. We also showed that the formation of TTR-IDIF complex enhances brain penetration of both TTR and IDIF [46]. Additionally, recent isothermal titration calorimetry (ITC) studies have provided the structural basis of the chaperoning effect of

IDIF on the TTR/A β complex formation, and have confirmed that not all TTR tetramer stabilizers behave as small-molecule chaperones (SMCs) of the TTR/A β interaction [47]. These results encouraged further *in vivo* investigation of possible therapeutic efficacy of IDIF. Furthermore, a screening process on small TTR-stabilizers recently conducted in our group showed that the drug tolcapone (Figure 1), a good TTR stabilizer clinically used for the treatment of TTR-related amyloidosis [48, 49], has not chaperoning activity on the TTR/A β interaction, which consequently may serve as a good control drug to shed light on the contribution of both TTR-stabilizing and chaperoning properties on therapeutic efficacy.

Here, we present longitudinal and long term (5–14 months of age) *in vivo* evaluation of the therapeutic efficacy of IDIF and tolcapone in AD transgenic mice (A β PP^{swe}/PS1A246E/TTR+/-). The treatment efficacy was determined based on the differences in the levels of A β between the treated and non-treated groups. Non-invasive, ultra-sensitive *in vivo* imaging technique, Positron Emission Tomography (PET), using validated radiotracer [¹⁸F]florbetaben, was used as a surrogate of A β deposition, based on its previous success in A β imaging in AD patients [50] and different transgenic AD mouse models [51-56].

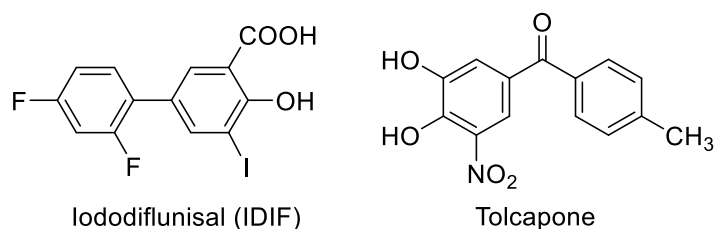


Figure 1. TTR tetramer stabilizers: small-molecule compounds iododiflunisal (IDIF) and tolcapone.

2. Methods

2.1 Compounds

IDIF meglumine salt was prepared as previously described [45]. In brief, to a solution of *N*-methyl-D-glucamine (meglumine) (1.22 g, 6.23 mmol) in water (2 mL), ethanol (0.5 mL) and IDIF (2.34 g, 4.23 mmol) were added over 15 min in small portions. The solution was stirred for 2 h, evaporated under reduced pressure and frozen. Tolcapone was isolated from the registered drug Tasmar (MEDA Pharma). In brief, the pills were triturated in the presence of ethyl acetate. The solution was filtered, and the filtrate evaporated under reduced pressure. The corresponding meglumine salt was prepared in the same way as reported for IDIF meglumine salt. Purity of all final compounds was proved to be $\geq 95\%$ by means of high-performance liquid chromatography (HPLC), high-resolution mass spectrometry (HR-MS) and nuclear magnetic resonance (NMR) spectroscopy.

2.2 Radiolabeling

[^{18}F]Florbetaben was prepared by ^{18}F -fluorination/hydrolysis of the *N*-Boc-protected precursor as previously described [57] with minor modifications. The radiosynthesis was performed using a TRACERlab FX_{FN} synthesis module (GE Healthcare). [^{18}F]F⁻ was first trapped on a pre-conditioned Sep-Pak® Accell Plus QMA Light cartridge (Waters, Milford, MA, USA), and then eluted with a solution of Kryptofix K_{2.2.2}/K₂CO₃ in a mixture of water and acetonitrile. After complete elimination of the solvent by azeotropic evaporation, a solution containing the precursor (3 mg) in dimethylsulfoxide (1 mL) was added and the mixture was heated at 165 °C for 5 min. The reactor was then cooled at room temperature, 10% HCl aqueous solution was added (0.25 mL) and the mixture was heated (2.5 min, 90 °C). The reaction crude was then diluted with NaOH solution (0.33

mL, 0.1 g/mL) and 3 mL of mobile phase (see below), and purified by high performance liquid chromatography (HPLC) using a Nucleosil 100-7 C18 column (Macherey-Nagel, Düren, Germany) as stationary phase and aqueous ascorbate buffer solution (20 g of ascorbic acid + 4.54 g NaOH in 2 L water, pH adjusted to 8.7 with 0.1 M NaOH; this solution diluted 1:1 with water)/acetonitrile (40/60, v/v) as the mobile phase at a flow rate of 5 mL/min. The desired fraction (retention time = 29–30 min) was collected, diluted with water (20 mL), and the radiotracer was retained on a C-18 cartridge (Sep-Pak® Light, Waters, Milford, MA, USA) and further eluted with ethanol (1 mL) and ascorbate buffer solution (20 g of ascorbic acid + 4.54 g NaOH in 2 L water, pH adjusted to 8.7 with 0.1 M NaOH; 5 mL). Filtration through a 0.22 µm filter yielded the final solution, ready for injection. Chemical and radiochemical purity and molar activity were determined by HPLC using an Agilent 1200 Series system equipped with a radioactivity detector (Gabi, Raytest) and a variable wavelength detector ($\lambda = 350$ nm) connected in series. A RP-C18 column (Mediterranea Sea 18, 4.6×150 mm, 5 µm particle size; Teknokroma, Spain) was used as the stationary phase and ascorbate buffer solution (20 g of ascorbic acid + 4.54 g NaOH in 2 L water, pH adjusted to 8.7 with 0.1 M NaOH; this solution diluted 1:1 with water)/acetonitrile (40/60, v/v) as the mobile phase (retention time = 5.4 min).

2.3 Animals and study design

Animals were maintained and handled in accordance with the Guidelines for Accommodation and Care of Animals (European Convention for the Protection of Vertebrate Animals Used for Experimental and Other Scientific Purposes). All animal procedures were performed in accordance with the European Union Animal Directive

(2010/63/EU). Experimental procedures were approved by the corresponding Ethical Committees.

The mouse model A β PPswe/PS1A246E/TTR+/- (carrying only one copy of the TTR gene), was generated as previously described [45] by crossing A β PPswe/PS1A246E transgenic mice [58] (B6/C3H background) purchased from The Jackson Laboratory with TTR-null mice (TTR-/-) (SV129 background) [59]. Mice were bred at I3S (Porto, Portugal) and a randomly selected cohort of females (n=21) was transferred to CIC biomaGUNE (San Sebastian, Spain) at 4–5 months of age to apply treatments and conduct imaging studies. Upon arrival, mice were randomly divided into three groups: Group I, non-treated (control; n=7); group II, IDIF-treated (n=7); and group III, tolcapone-treated (n=7) mice. The treatment was introduced in the drinking water at a concentration of 575 mg of meglumine IDIF salt and 575 mg meglumine tolcapone salt per liter (2.8 mg drug/rodent/day).

The disease progression was followed using PET-[¹⁸F]florbetaben at the age of 5 (n=21), 9 (n=21), 11 (n=20) and 14 months (n=19). One of the animals (group III) was not injected properly at the age of 11 months, and all the activity was found in the tail. One of the animals (group I) died at the age of 12 months and could not be submitted to the last imaging session. Another animal (group II) presented a damaged tail at the age of 14 months and administration of the tracer was not possible. All the animals were sacrificed at the age of 14 months, after being submitted to the last imaging session. The low mortality rate observed is in agreement with our previous experience with this model.

2.4 PET-CT imaging

Imaging experiments were performed using an eXplore Vista-CT small animal PET-CT system (GE Healthcare). In all cases, anaesthesia was induced with 3–5% isoflurane in pure oxygen and maintained during imaging studies with 1.5–2.0% isoflurane in pure oxygen. Mice were injected intravenously (IV) with [¹⁸F]florbetaben (9.5–20.5 MBq; injected volume: 100–150 μL). At each time point, a 30-min static PET image was acquired 30 min post IV injection in one bed position to assess the accumulation in the brain (energy range 400–700 keV). A CT scan was acquired immediately after PET acquisition (X-Ray energy: 40 kV, intensity: 140 μA). PET images were reconstructed using filtered back projection (FBP) applying random, scatter, and attenuation corrections.

PET images were co-registered with a magnetic resonance imaging (MRI) template (M. Mirrione-T2, available in the π-MOD image processing tool) and different brain regions (the cortex, the hippocampus and the cerebellum) were automatically delineated. The concentration of activity was determined in each region and expressed as Standard Uptake Value (SUV). Treatment efficacy was determined based on the amount of [¹⁸F]florbetaben in different brain regions. The hippocampus (HIP) and the cortex (CTX) were chosen as brain regions of interest. The cerebellum (CB) was chosen as reference region. Aβ plaque abundance was determined as relative SUV (SUVr) of [¹⁸F]florbetaben in HIP and CTX with respect to CB.

For voxel-by-voxel analysis, SUVr images for the individual animals within each group at the ages of 5 and 11 months were averaged. For each of the groups, the resulting averaged images at the ages of 11 and 5 months were divided on a voxel-by-voxel basis, and the histograms for the HIP and the CTX were obtained.

2.5 Immunohistochemical analysis

A β plaque burden was evaluated by performing free-floating immunohistochemistry assay on 30 μ m-thick cryostat coronal brain sections (5 slices per animal, ranging from Bregma -1.2 to -3.2), using monoclonal biotinylated A β 1-16 antibody (6E10) (Covance Research Products, Inc.), as previously described [60]. In brief, free-floating brain sections were washed twice in phosphate-buffered saline (PBS), and once in distilled water (dH₂O). For partial amyloid denaturation, 70% formic acid (FA) was used for 15 min at room temperature, with gentle agitation. After washing in dH₂O and then PBS, endogenous peroxidase activity was inhibited with 1% hydrogen peroxide (H₂O₂) in PBS for 20 min. Following PBS washes, sections were blocked in blocking solution (10% fetal bovine serum (FBS) and 0.5% Triton X-100) for 1 h at room temperature and then incubated with biotinylated 6E10 primary antibody overnight at 4 °C, with gentle agitation. Sections were washed with PBS and incubated in Vectastain® Elite ABC Reagent (Vector Laboratories, Inc.). After washing once more with PBS, sections were developed with diaminobenzidine (Sigma-Aldrich, Inc.), mounted on 0.1% gelatin-coated slides and dried overnight at room temperature. After dehydration, slides were coverslipped under Entellan® (Merck & Co., Inc.) and examined using an Olympus BX50 light microscope. Plaque burden was evaluated using Image-Pro Plus software, by analyzing the immunostained area fraction in the HIP and CTX, separately, after delimitation of the respective regions in each of the five sections (slices) analysed per animal. A β plaque burden is expressed as the percentage of the stained area relative to the total area of the respective brain region.

2.6 Statistical analysis

Statistical significance of differences in between time points (for each treatment) or treatment (at a single time point) was calculated using repeated measures 2-way

ANOVA analysis. Differences were concluded significant for P values < 0.05: P < 0.05, *; P < 0.01, **, P < 0.001, ***; and P < 0.0001, ****. All data are presented as individual values, including mean values and min-to-max ranges. Statistical tests were performed in GraphPad Prism 7.03 (GraphPad Software, CA, USA).

3. Results

3.1 Radiochemistry

The radiotracer [¹⁸F]florbetaben was synthesized in overall non-decay corrected radiochemical yield of 17±7%. Radiochemical purity as determined by radio-HPLC was > 95% in all cases at the injection time, and no major peaks were identified in the UV chromatographic profiles, confirming the chemical purity (see ESI, Fig. S2 for representative chromatograms). Molar activity values at the end of the synthesis were in the range 184-534 GBq/μmol. Because each synthesis was used to image different animals consecutively, the mass dose of the radiotracer that was administered to the animals differed from the first to the last animal within one day. However, the order of scanning was randomized in order to keep the average injected dose (both in terms of amount of radioactivity and molar amount) constant along groups and ages. Complete information about the amount of radioactivity and mass dose administered to each individual animal at each time point are included in Table S2 (see ESI).

3.2 PET-CT imaging

Longitudinal PET-CT imaging using [¹⁸F]florbetaben was carried out to determine the Aβ plaque burden in selected brain sub-regions *in vivo*. Animals submitted to different treatments were scanned at 5, 9, 11 and 14 months of age. SUVr values (determined as the ratio between SUV values in the investigated region and CB) in CTX progressively increased with age, irrespective of the treatment received by the animals (Figure 2a).

SUVr values in CTX were always below 1, indicating that the radiotracer uptake in this brain region was actually lower than the uptake in CB. Between-age difference within each group was significant only for non-treated animals ($P=0.0229$ for 14 months vs. 5 months), but no statistical significance in increase of $A\beta$ load between 5 and 14 months was observed in IDIF- and tolcapone-treated groups ($P=0.147$ and 0.056 , respectively). Differences in SUVr between groups at a given age were not significant.

In contrast, SUVr values determined for HIP showed significant differences between groups (Figures 2b and 2c). For non-treated animals, values progressively increased from age=5 months (0.98 ± 0.04) to age=11 months (1.06 ± 0.03 ; $P=0.0002$) and stabilized afterwards (1.07 ± 0.03 at age=14 months; $P<0.0001$ vs. SUVr at age=5 months). For IDIF-treated animals, the trend was different. Values raised from 0.98 ± 0.03 at age=5 months to 1.00 ± 0.03 at age=11 months (non-significant increase, $P=0.455$), and dramatically increased afterwards to reach a value of 1.07 ± 0.02 at the age of 14 months ($P=0.0005$ vs. SUVr at age=11 months; $P<0.0001$ vs. SUVr at age=5 months). Finally, tolcapone-treated animals showed a trend that laid in between those observed for non-treated and IDIF-treated animals. For this group, values progressively increased with time, resulting in SUVr values 0.97 ± 0.04 , 1.01 ± 0.03 , 1.03 ± 0.02 and 1.065 ± 0.015 at 5, 9, 11 and 14 months, respectively. Noteworthy, SUVr values obtained at 11 and 14 months significantly differ from those obtained at 5 months ($P=0.0024$ and <0.0001 , respectively). At the age of 11 months, SUVr values obtained for IDIF-treated animals (1.00 ± 0.03) are significantly lower than those obtained for non-treated animals (1.06 ± 0.03 ; $P=0.0088$) (see Figure 3a for representative images). The differences observed in the hippocampus among groups were also evident on the images obtained by subtracting, voxel-by-voxel, the brain image at 5 months of age from the images of the same animal at 9, 11, and 14 months of age (Figure 3b).

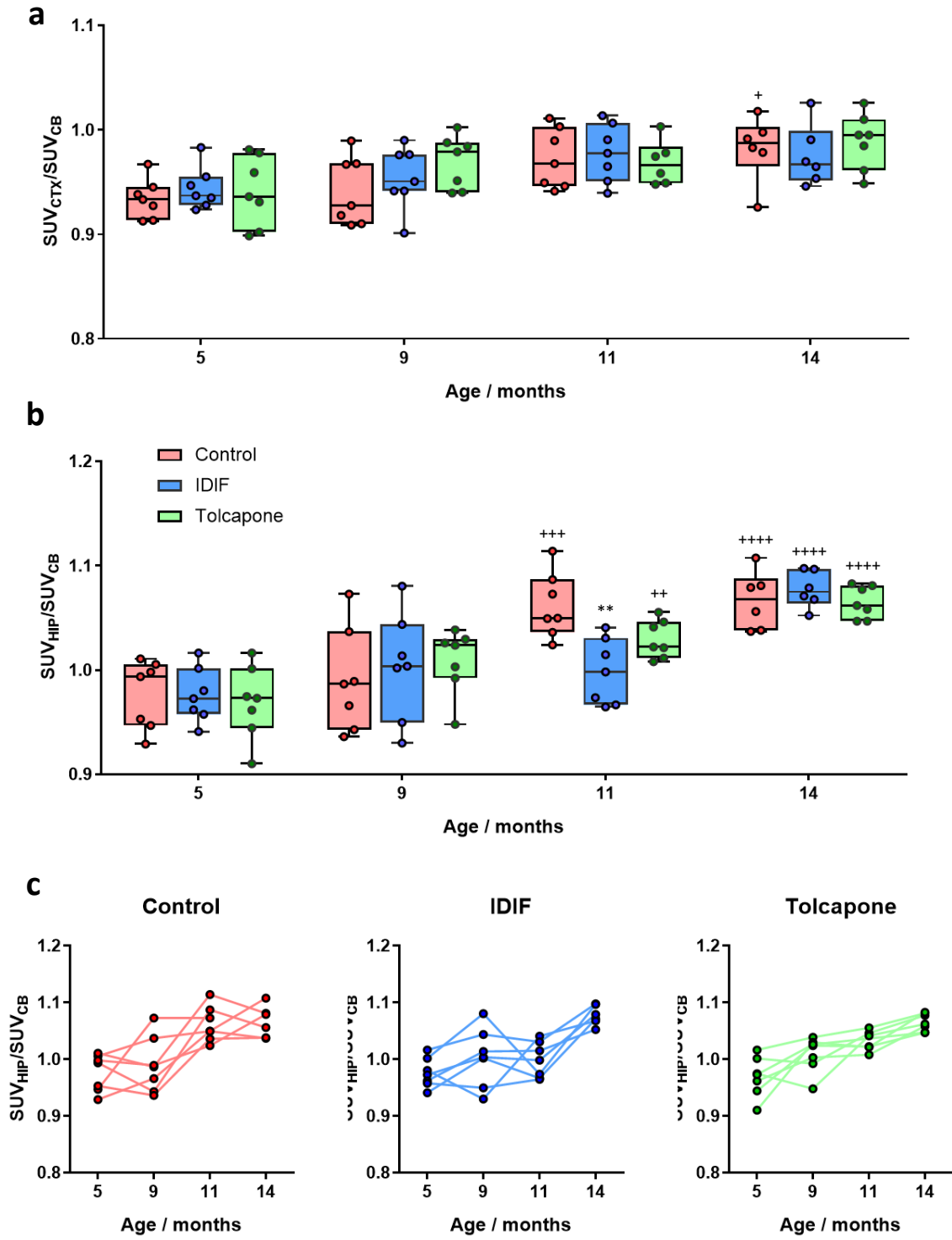


Figure 2. (a, b) SUVR values (SUV values relative to CB) in CTX (a) and HIP (b), obtained after administration of [¹⁸F]florbetaben to control, IDIF-treated and tolcapone-treated mice at different ages. Dots represent values for individual mouse; probability values for differences of each value with respect to the same group at age=5 months are depicted as +(P<0.05), ++

($P < 0.01$), +++ ($P < 0.001$), and ++++ ($P < 0.0001$); probability values for differences between treated groups and the control group at a given time point are depicted as ** ($P < 0.01$); (c) SUVr values (SUV values relative to CB) in HIP, obtained after administration of [^{18}F]florbetaben to control, IDIF-treated and tolcapone-treated mice at different ages. Connected individual values correspond to the same animal.

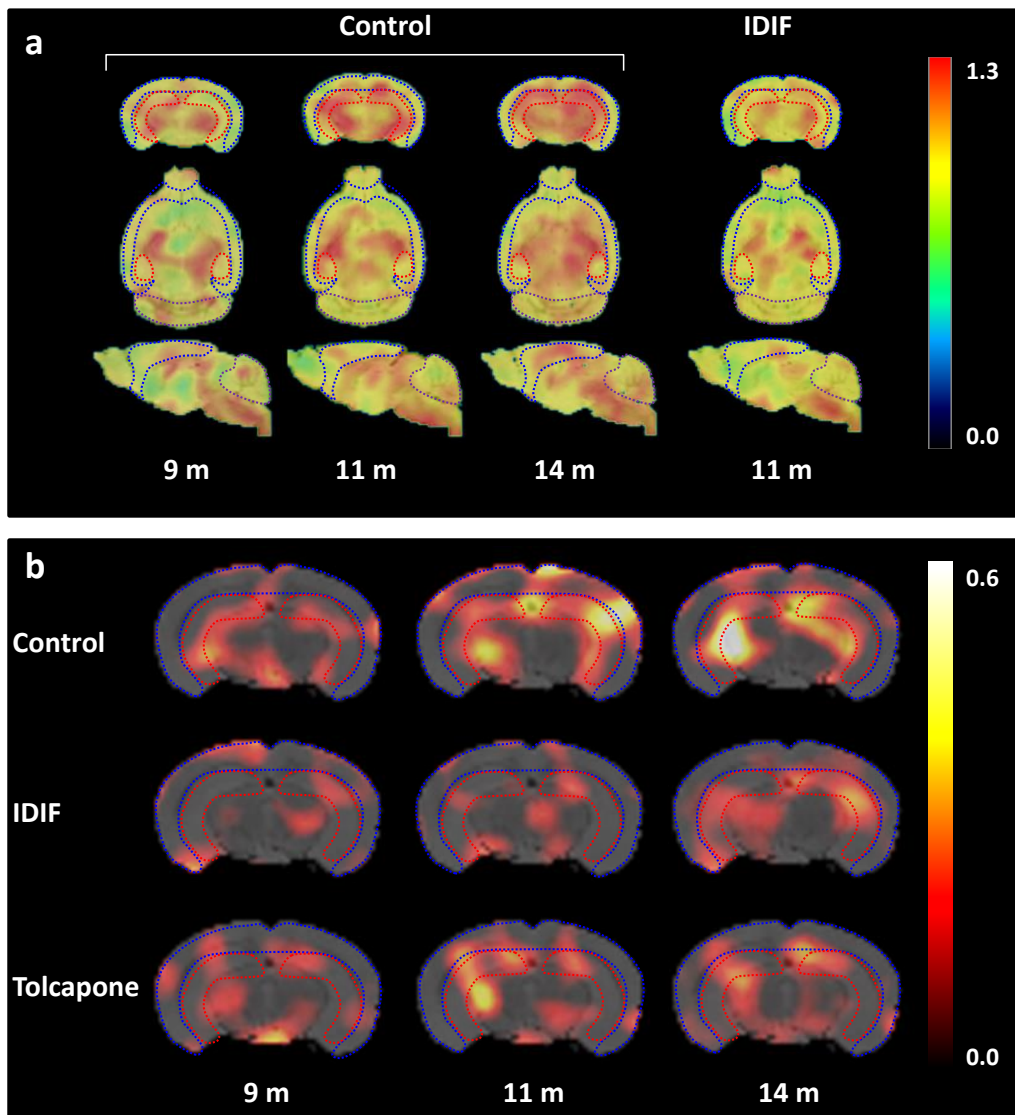


Figure 3. (a) Representative axial (top), coronal (middle) and sagittal (bottom) PET images corresponding to a control animal at ages=9, 11 and 14 months, and IDIF-treated mouse at the age of 11 months. PET images show SUVr values (values relative to CB) and have been co-registered with a brain mouse atlas. Volumes of interest drawn in CTX (blue), HIP (red) and CB

(brown) are displayed; (b) representative axial PET images corresponding to control, IDIF-treated and tolcapone-treated animals at ages=9, 11 and 14 months, representing, voxel-by-voxel, increased SUVR values with respect to the value at the age of 5 months for the same animal. PET images have been co-registered with a mouse brain atlas. Volumes of interest drawn in CTX (blue) and HIP (red) are displayed on each image.

3.3 Immunohistochemistry

The effect of the treatment on A β deposition was studied by assessing A β burden in all animals after the last imaging session (age=14 months) by IHC analyses followed by quantification. IHC did not show any significant differences between treated and non-treated animals at this time point, neither in CTX (Figure 4a) nor in HIP (Figure 4b). In all cases, high plaque density was observed, with significant variability among individuals, as observed in the photomicrographs (Figure 4c).

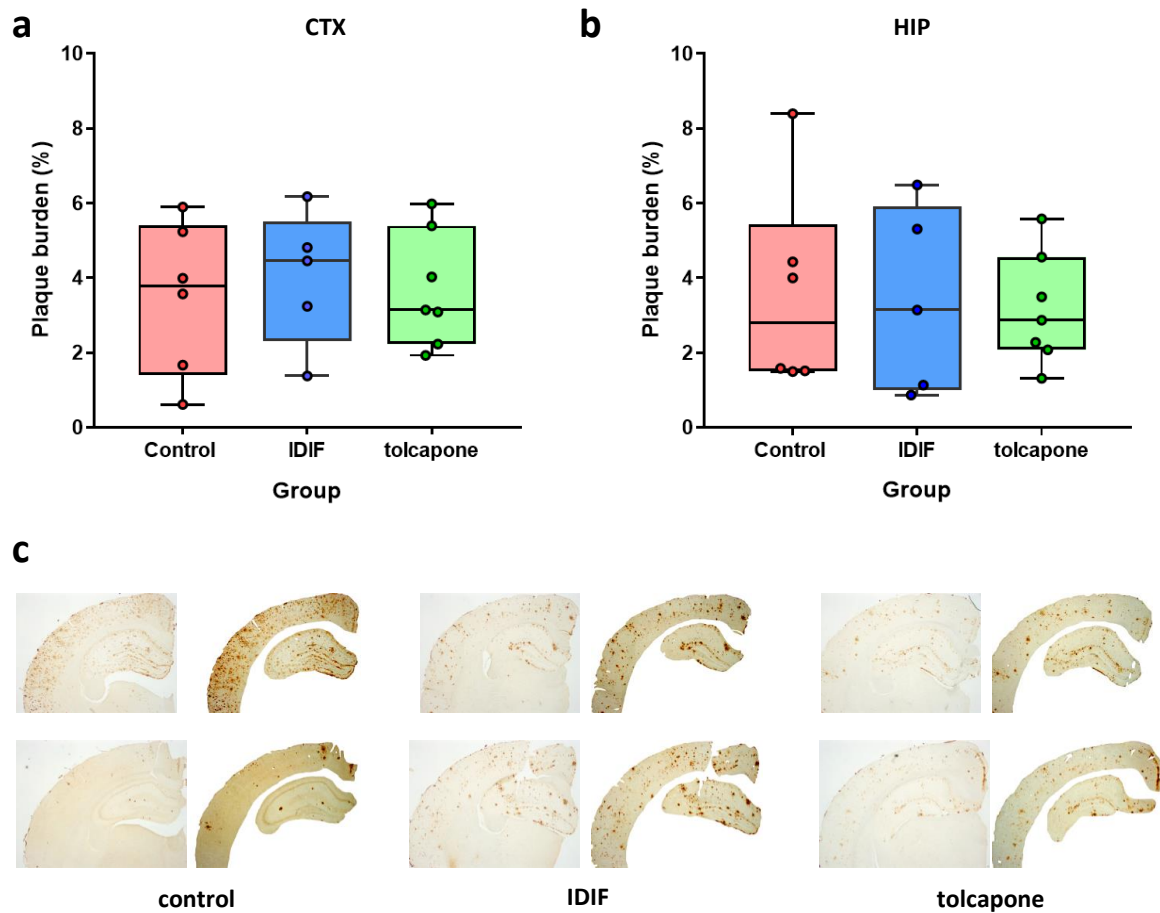


Fig. 4. (a, b) A β plaque burden in CTX and HIP of control, IDIF-treated (IDIF) and tolcapone-treated (tolcapone) mice at age=14 months. Dots represent individual values; (c) photomicrographs illustrate immunohistochemical analysis of brain A β plaques using the 6E10 antibody. Brain slices (left) and selected areas for quantification (right) are shown. Slides within each group correspond to two representative animals.

4. Discussion

TTR is an important transporter protein for the brain defense against pathophysiological stress caused by A β deposition, as demonstrated in AD mouse models. Overexpression of human TTR in AD mice results in protection against A β deposition and toxicity [29], whereas deletion of the of the endogenous TTR gene results

in more severe disease [29, 60, 61]. Although some studies reported that mouse wild type (wt) TTR, which is more stable than human wt TTR, is less capable of preventing A β aggregation and oligomers toxicity [62-64], *in vivo* studies show accelerated development of the neuropathologic phenotype when the endogenous TTR gene is deleted, demonstrating that the mouse TTR has a relevant effect on the disease progression in AD mouse models [29, 60, 61]. This justifies the use of mouse models for the investigation of the effects of TTR stability on amyloidosis and the significance of these results for putative translation into humans.

Previous studies in AD animal models carried out by our research group have shown that oral administration of IDIF results in decreased A β plaque deposition and ameliorates cognitive status at early stages of the disease [45]. These results favor the hypothesis that TTR tetramer is actually the suppressor of A β aggregation *in vivo*, as suggested also by other authors [38].

To fully evaluate the potential of IDIF to act as a disease-modifying drug in AD, longitudinal therapeutic efficacy and long-term treatment effect on plaque deposition were assessed by [18 F]florbetaben amyloid-PET imaging. Comparative studies were also performed with another TTR tetramer stabilizer, the drug tolcapone. This FDA-approved molecule for Parkinson's disease is capable to penetrate the BBB [65] and is currently being repurposed for the treatment of hereditary TTR amyloidosis (ATTR) [48, 49] and CNS amyloidosis [49].

Similar to previous preclinical PET-[18 F]florbetaben studies [51-53, 55], SUVr values were used to evaluate plaque density in different brain regions. Plaque density was determined in CTX and HIP, areas that are the most affected by A β deposition in the animal model used for this study. SUVr values in CTX and HIP of non-treated animals

progressively increased with animal age (Figures 2a–2b). Similar to previously reported studies in a different animal model [52], more profound differences in SUVr were observed in HIP than in CTX. PET images obtained at 9, 11 and 14 months (Figure 3a) clearly showed an increase in SUVr values in HIP of non-treated animals from 9 to 11 months, while the increase in plaque load from 11 to 14 months was not apparent, according to quantification data.

As for the treatment groups, IDIF-treatment delayed A β plaque build-up in HIP until the age=11 months, but did not affect plaque accumulation at the final stage of the disease. IHC analysis at the end point confirmed that there were no significant differences between IDIF-treated and non-treated animal groups (Figure 4). The factors behind the sudden increase in the plaque load in IDIF-group at the final point of the study are unknown. The possible reasons behind these unexpected results could be a consequence of experimental flaws, physiological changes or changes in disease mechanism. The factors such as decrease in fluid intake as a consequence of the phenotype (which has been reported for other AD models [66]) or hindered mobility, which may lead to lower drug intake, could limit therapeutic efficacy. Occurrence of other disease-related processes that possibly take over the main role at more advanced stages of the disease and the inability of TTR tetramer to take its primary role in the late stages of the disease are also not excluded. The reasons behind these changes are beyond the scope of this work and will be addressed in future studies.

The positive IDIF treatment effect observed in HIP was not matched in CTX, suggesting that CTX was not affected by any of the treatments. However, the cortex is a relatively large region and plaque deposition might be heterogeneous. Hence, we decided to explore local differences within this region and extended our investigation to the

hippocampus. With that aim, SUVR images for all individual animals obtained at the age of 5 and 11 months were averaged, and the ratio 11-to-5 months was calculated for each group in a voxel-by-voxel fashion. Histograms revealed quasi-perfect Gaussian distribution in the case of the CTX (see ESI, Figure S3) with almost overlapped mean values, thus confirming that no regional uptake within the cortex is present. Contrarily, Gaussian curves fitted to the histograms corresponding to the HIP show increased mean values for tolcapone and control groups, in agreement with our quantification data. Noteworthy, the histogram for IDIF-treated group shows an asymmetric profile, probably suggesting that in spite of the protective effect of IDIF, A β plaques could be present in certain sub-regions of the hippocampus at the age of 11 months.

One of the possible reasons behind the lack of treatment effect in the CTX could be differences in the amount of TTR in different brain regions, as reported previously [67]. Furthermore, our recent PET-imaging study shows that entrance of TTR into the brain after intravenous administration starts at the third ventricles, which suggests that TTR traffic occurs partially via the blood-cerebrospinal fluid barrier (BCSFB) and not only through the blood brain barrier (BBB) [46]. Ultimately, this led to lower and delayed TTR presence in peripheral areas of the brain [46], such as CTX, where a significant concentration of TTR could be observed only at 6 hours after administration. Assuming the same transport mechanism of IDIF- and tolcapone-stabilized TTR, this delay could be one of the reasons for insufficient influx of the complex into CTX. In turn, this would lead to ineffective A β clearance, resulting in the absence of differences between treated and non-treated mice.

No clear evidence of A β protein clearance was observed in the tolcapone-treated group. Compared to non-treated animals, tolcapone helped slow down the rate of plaque

deposition in HIP, suggesting some protective effects of the treatment. Even though previous reports showed that tolcapone and entacapone inhibit A β fibrilization in a specific and concentration-dependent manner [68], our results suggest that, at the assayed dose, direct effect of tolcapone was not sufficient to produce significant differences between treated and non-treated animals.

Difference in effectiveness between IDIF and tolcapone suggests a different mechanism of action. In recent studies, we have demonstrated that, contrarily to IDIF, the orphan drug Tafamidis and the drug diflunisal (NSAID), both TTR tetramer stabilizers, do not show chaperoning capabilities of TTR/A β interaction [47]. Evidence for the lack of chaperoning effect of tolcapone in the TTR/A β interaction has been also observed using similar calorimetric studies (See ESI, Figure S1 and Table S1). Hence, limited chaperoning ability in TTR/A β interaction could be the cause of the inability of tolcapone-TTR complex to promote A β clearance from the brain.

Our study presents positive and promising results; however, it has some caveats worth to be mentioned. First, animal studies were only performed in females, while a thorough analysis of therapeutic efficacy may require the use of both genders. The animal model used in this study shows gender-associated modulation of brain A β levels by TTR, and females present a more severe AD-like neuropathology [60]. Because of this, and also considering that women are more affected than men by AD, we decided to carry out our proof of concept studies only in females. Future studies should incorporate both males and females, in order to explore inter-gender differences in therapeutic efficacy.

The second limitation is the lack of longitudinal information regarding IHC analysis. Inclusion of extra animals to be sacrificed at 5, 9, and 11 months of age to correlate A β plaque burden in different brain sub-regions with imaging data would have been highly

desirable to further support our *in vivo* results. Still, the use of a validated imaging modality and radiotracer supports the reliability of our results.

Finally, administering the drug in the drinking water is probably not optimal, as heterogeneous water intake may lead to variations in drug exposition and consequently also in therapeutic efficacy. Still, for such long-term treatments (total duration of ca. 10 months) other alternatives present severe limitations. Repeated oral gavage can affect animal health and welfare [69]. Intraperitoneal delivery has questionable accuracy [70], and repeated administration can result in a cumulative irritant effect and needle-induced damage. Refined alternatives such as using drug-loaded chows present similar limitations to the method using in our work. In all cases, the evaluation of drug-plasma levels may aid in better correlating exposure levels with pharmacodynamics measurements.

In spite of the above-mentioned limitations, our results position IDIF as a potential disease-modifying drug for AD, and encourage follow-up studies that will include investigation of both males and females, dose-response studies, evaluation of other SMCs of the TTR/A β interaction and translation to larger animal species.

5. Conclusions

In conclusion, this is the first large-scale longitudinal A β -PET study of cerebral amyloidosis in a transgenic AD mouse model treated with IDIF, a small-molecule compound that enhances the TTR/A β interaction. Our work confirms positive effects of IDIF on the delay of A β deposition in the hippocampus. This study offers an insight into the possible effect of stabilization of TTR complexes on the degree of A β amyloidosis in the brain longitudinally. It also offers the first *in vivo* evidence of the importance of chaperoning ability on A β deposition. Although further studies are needed, these

preliminary results suggest that IDIF is a valuable candidate for amelioration of A β aggregate-related pathological stress in the CNS. This research shows the great significance of development of small-molecule chaperones as potential disease modifying drugs for AD therapeutics and provides the basis for the design of further investigations, including dose-response studies and translation of this new disease-modifying approach to clinical trials for AD therapy.

ACKNOWLEDGEMENTS

The work was supported by a grant from the Fundació Marató de TV3 (Neurodegenerative Diseases Call, Project Reference 20140330-31-32-33-34, <http://www.ccma.cat/tv3/marato/en/projectes-financats/2013/212/>). The group at CIC biomaGUNE also acknowledges The Spanish Ministry of Economy and Competitiveness for funding through Grant CTQ2017-87637-R. I. Cardoso worked under the Investigator FCT Program which is financed by national funds through the Foundation for Science and Technology (FCT, Portugal) and co-financed by the European Social Fund (ESF) through the Human Potential Operational Programme (HPOP), type 4.2 - Promotion of Scientific Employment. G. Arsequell also acknowledges financial support from the Spanish Ministry of Economy (CTQ2016-76840-R). E.Y. Cotrina acknowledges a contract from Fundació Marató de TV3, Spain (Project ref. 20140330-31-32-33-34) and a one year contract from Ford-Fundación Apadrina la Ciencia. Part of the work was conducted under the Maria de Maeztu Units of Excellence Programme – Grant No. MDM-2017-0720. The authors thank the animal facility staff at CIC biomaGUNE for administration of the compounds; Aitor Lekuona and Víctor Salinas for assistance in cyclotron operation and automated syntheses; and Prof. Dr. Alfredo Ballesteros (University of Oviedo, Oviedo, Spain) for support on the IDIF synthesis. G.

Arsequell from IQAC-CSIC acknowledges Dr. Rafel Prohens from Unitat de Polimorfisme i Calorimetria, Centres Científics i Tecnològic (University of Barcelona) for his supervision and assistance in ITC studies.

CONFLICT OF INTEREST

The authors have no conflict of interest to report

REFERENCES

- [1] (2019) 2019 Alzheimer's disease facts and figures. *Alzheimer's & Dementia* **15**, 321-387.
- [2] Selkoe DJ, Hardy J (2016) The amyloid hypothesis of Alzheimer's disease at 25 years. *EMBO Mol Med* **8**, 595-608.
- [3] Goedert M, Spillantini MG, Cairns NJ, Crowther RA (1992) Tau proteins of Alzheimer paired helical filaments: abnormal phosphorylation of all six brain isoforms. *Neuron* **8**, 159-168.
- [4] Forner S, Baglietto-Vargas D, Martini AC, Trujillo-Estrada L, LaFerla FM (2017) Synaptic Impairment in Alzheimer's Disease: A Dysregulated Symphony. *Trends Neurosci* **40**, 347-357.
- [5] McGeer EG, McGeer PL (2003) Inflammatory processes in Alzheimer's disease. *Prog Neuropsychopharmacol Biol Psychiatry* **27**, 741-749.
- [6] Koizumi K, Wang G, Park L (2016) Endothelial Dysfunction and Amyloid-beta-Induced Neurovascular Alterations. *Cell Mol Neurobiol* **36**, 155-165.
- [7] Cao J, Hou J, Ping J, Cai D (2018) Advances in developing novel therapeutic strategies for Alzheimer's disease. *Molecular Neurodegeneration* **13**, 64.

- [8] Cummings J (2018) Lessons Learned from Alzheimer Disease: Clinical Trials with Negative Outcomes. *Clin Transl Sci* **11**, 147-152.
- [9] Cummings J, Lee G, Ritter A, Sabbagh M, Zhong K (2019) Alzheimer's disease drug development pipeline: 2019. *Alzheimer's and Dementia: Translational Research and Clinical Interventions* **5**, 272-293.
- [10] Cummings J, Ritter A, Zhong K (2018) Clinical Trials for Disease-Modifying Therapies in Alzheimer's Disease: A Primer, Lessons Learned, and a Blueprint for the Future. *J Alzheimers Dis* **64**, S3-S22.
- [11] Molinuevo JL, Minguillon C, Rami L, Gispert JD (2018) The Rationale behind the New Alzheimer's Disease Conceptualization: Lessons Learned during the Last Decades. *Journal of Alzheimer's Disease* **62**, 1067-1077.
- [12] Mehta D, Jackson R, Paul G, Shi J, Sabbagh M (2017) Why do trials for Alzheimer's disease drugs keep failing? A discontinued drug perspective for 2010-2015. *Expert Opinion on Investigational Drugs* **26**, 735-739.
- [13] Cummings J, Feldman HH, Scheltens P (2019) The "rights" of precision drug development for Alzheimer's disease. *Alzheimer's Research and Therapy* **11**.
- [14] Mannini B, Cascella R, Zampagni M, Van Waarde-Verhagen M, Meehan S, Roodveldt C, Campioni S, Boninsegna M, Penco A, Relini A, Kampinga HH, Dobson CM, Wilson MR, Cecchi C, Chiti F (2012) Molecular mechanisms used by chaperones to reduce the toxicity of aberrant protein oligomers. *Proc Natl Acad Sci U S A* **109**, 12479-12484.
- [15] Narayan P, Meehan S, Carver JA, Wilson MR, Dobson CM, Klenerman D (2012) Amyloid- β oligomers are sequestered by both intracellular and extracellular chaperones. *Biochemistry (Mosc)* **51**, 9270-9276.

- [16] Cohen SIA, Arosio P, Presto J, Kurudenkandy FR, Biverstål H, Dolfe L, Dunning C, Yang X, Frohm B, Vendruscolo M, Johansson J, Dobson CM, Fisahn A, Knowles TPJ, Linse S (2015) A molecular chaperone breaks the catalytic cycle that generates toxic A β oligomers. *Nature Structural and Molecular Biology* **22**, 207-213.
- [17] Arosio P, Michaels TCT, Linse S, Månsson C, Emanuelsson C, Presto J, Johansson J, Vendruscolo M, Dobson CM, Knowles TPJ (2016) Kinetic analysis reveals the diversity of microscopic mechanisms through which molecular chaperones suppress amyloid formation. *Nature Communications* **7**.
- [18] Watts G (2018) Prospects for dementia research. *Lancet (London, England)* **391**, 416.
- [19] Ji L, Zhao X, Hua Z (2015) Potential therapeutic implications of gelsolin in Alzheimer's disease. *Journal of Alzheimer's Disease* **44**, 13-25.
- [20] Nelson AR, Sagare AP, Zlokovic BV (2017) Role of clusterin in the brain vascular clearance of amyloid-beta. *Proc Natl Acad Sci U S A* **114**, 8681-8682.
- [21] Beeg M, Stravalaci M, Romeo M, Carra AD, Cagnotto A, Rossi A, Diomedede L, Salmona M, Gobbi M (2016) Clusterin Binds to Abeta1-42 Oligomers with High Affinity and Interferes with Peptide Aggregation by Inhibiting Primary and Secondary Nucleation. *J Biol Chem* **291**, 6958-6966.
- [22] Wisniewski T, Drummond E (2020) APOE-amyloid interaction: Therapeutic targets. *Neurobiol Dis* **138**, 104784.
- [23] Boada M, Anaya F, Ortiz P, Olazarán J, Shua-Haim JR, Obisesan TO, Hernandez I, Muñoz J, Buendía M, Alegret M, Lafuente A, Tarraga L, Nunez L, Torres M, Grifols JR, Ferrer I, Lopez OL, Paez A (2017) Efficacy and Safety of Plasma Exchange with 5% Albumin to Modify Cerebrospinal Fluid and Plasma Amyloid-beta

- Concentrations and Cognition Outcomes in Alzheimer's Disease Patients: A Multicenter, Randomized, Controlled Clinical Trial. *J Alzheimers Dis* **56**, 129-143.
- [24] Algamal M, Ahmed R, Jafari N, Ahsan B, Ortega J, Melacini G (2017) Atomic-resolution map of the interactions between an amyloid inhibitor protein and amyloid beta (A β) peptides in the monomer and protofibril states. *J Biol Chem* **292**, 17158-17168.
- [25] Boada M, López O, Núñez L, Szczepiorkowski ZM, Torres M, Grifols C, Páez A (2019) Plasma exchange for Alzheimer's disease Management by Albumin Replacement (AMBAR) trial: Study design and progress. *Alzheimer's and Dementia: Translational Research and Clinical Interventions* **5**, 61-69.
- [26] Sabbagh MN (2020) Alzheimer's Disease Drug Development Pipeline 2020. *The Journal of Prevention of Alzheimer's Disease* **7**, 66-67.
- [27] Schwarzman AL, Gregori L, Vitek MP, Lyubski S, Strittmatter WJ, Enghilde JJ, Bhasin R, Silverman J, Weisgraber KH, Coyle PK, et al. (1994) Transthyretin sequesters amyloid beta protein and prevents amyloid formation. *Proc Natl Acad Sci U S A* **91**, 8368-8372.
- [28] Stein TD, Johnson JA (2002) Lack of neurodegeneration in transgenic mice overexpressing mutant amyloid precursor protein is associated with increased levels of transthyretin and the activation of cell survival pathways. *Journal of Neuroscience* **22**, 7380-7388.
- [29] Buxbaum JN, Ye Z, Reixach N, Friske L, Levy C, Das P, Golde T, Masliah E, Roberts AR, Bartfai T (2008) Transthyretin protects Alzheimer's mice from the behavioral and biochemical effects of A β toxicity. *Proc Natl Acad Sci U S A* **105**, 2681-2686.
- [30] Alemi M, Gaitero C, Ribeiro CA, Santos LM, Gomes JR, Oliveira SM, Couraud PO, Weksler B, Romero I, Saraiva MJ, Cardoso I (2016) Transthyretin participates in

beta-amyloid transport from the brain to the liver- involvement of the low-density lipoprotein receptor-related protein 1? *Scientific Reports* **6**.

- [31] Gião T, Saavedra J, Cotrina E, Quintana J, Llop J, Arsequell G, Cardoso I (2020) Undiscovered roles for transthyretin: From a transporter protein to a new therapeutic target for Alzheimer's disease. *International Journal of Molecular Sciences* **21**.
- [32] Saraiva MJM (2001) Transthyretin amyloidosis: A tale of weak interactions. *FEBS Letters* **498**, 201-203.
- [33] Du J, Murphy RM (2010) Characterization of the interaction of β -Amyloid with Transthyretin monomers and tetramers. *Biochemistry (Mosc)* **49**, 8276-8289.
- [34] Li X, Zhang X, Ladiwala ARA, Du D, Yadav JK, Tessier PM, Wright PE, Kelly JW, Buxbaum JN (2013) Mechanisms of Transthyretin Inhibition of β -Amyloid Aggregation *In Vitro*. *The Journal of Neuroscience* **33**, 19423.
- [35] Jiang X, Smith CS, Petrassi HM, Hammarström P, White JT, Sacchettini JC, Kelly JW (2001) An engineered transthyretin monomer that is nonamyloidogenic, unless it is partially denatured. *Biochemistry (Mosc)* **40**, 11442-11452.
- [36] Garai K, Posey AE, Li X, Buxbaum JN, Pappu RV (2018) Inhibition of amyloid beta fibril formation by monomeric human transthyretin. *Protein Science* **27**, 1252-1261.
- [37] Nilsson L, Pamrén A, Islam T, Brännström K, Golchin SA, Pettersson N, Iakovleva I, Sandblad L, Gharibyan AL, Olofsson A (2018) Transthyretin Interferes with A β Amyloid Formation by Redirecting Oligomeric Nuclei into Non-Amyloid Aggregates. *Journal of Molecular Biology* **430**, 2722-2733.
- [38] Ghadami SA, Chia S, Ruggeri FS, Meisl G, Bemporad F, Habchi J, Cascella R, Dobson CM, Vendruscolo M, Knowles TPJ, Chiti F (2020) Transthyretin Inhibits Primary

- and Secondary Nucleations of Amyloid- β Peptide Aggregation and Reduces the Toxicity of Its Oligomers. *Biomacromolecules* **21**, 1112-1125.
- [39] Almeida MR, Gales L, Damas AM, Cardoso I, Saraiva MJ (2005) Small transthyretin (TTR) ligands as possible therapeutic agents in TTR amyloidoses. *Current Drug Targets: CNS and Neurological Disorders* **4**, 587-596.
- [40] Schwarzman AL, Tsiper M, Wente H, Wang A, Vitek MP, Vasiliev V, Goldgaber D (2004) Amyloidogenic and anti-amyloidogenic properties of recombinant transthyretin variants. *Amyloid* **11**, 1-9.
- [41] Ribeiro CA, Santana I, Oliveira C, Baldeiras I, Moreira J, Saraiva MJ, Cardoso I (2012) Transthyretin decrease in plasma of MCI and AD patients: Investigation of mechanisms for disease modulation. *Current Alzheimer Research* **9**, 881-889.
- [42] Alemi M, Silva SC, Santana I, Cardoso I (2017) Transthyretin stability is critical in assisting beta amyloid clearance– Relevance of transthyretin stabilization in Alzheimer's disease. *CNS Neuroscience and Therapeutics* **23**, 605-619.
- [43] Varamini B, Sikalidis AK, Bradford KL (2014) Resveratrol increases cerebral glycogen synthase kinase phosphorylation as well as protein levels of drebrin and transthyretin in mice: an exploratory study. *International Journal of Food Sciences and Nutrition* **65**, 89-96.
- [44] Santos LM, Rodrigues D, Alemi M, Silva SC, Ribeiro CA, Cardoso I (2016) Resveratrol administration increases transthyretin protein levels, ameliorating AD features: The importance of transthyretin tetrameric stability. *Mol Med* **22**, 597-607.
- [45] Ribeiro CA, Oliveira SM, Guido LF, Magalhaes A, Valencia G, Arsequell G, Saraiva MJ, Cardoso I (2014) Transthyretin stabilization by iododiflunisal promotes amyloid-beta peptide clearance, decreases its deposition, and ameliorates

- cognitive deficits in an Alzheimer's disease mouse model. *J Alzheimers Dis* **39**, 357-370.
- [46] Rios X, Gómez-Vallejo V, Martín A, Cossío U, Morcillo MÁ, Alemi M, Cardoso I, Quintana J, Jiménez-Barbero J, Cotrina EY, Valencia G, Arsequell G, Llop J (2019) Radiochemical examination of transthyretin (TTR) brain penetration assisted by iododiflunisal, a TTR tetramer stabilizer and a new candidate drug for AD. *Scientific Reports* **9**.
- [47] Cotrina EY, Gimeno A, Llop J, Jimenez-Barbero J, Quintana J, Valencia G, Cardoso I, Prohens R, Arsequell G (2020) Calorimetric studies of binary and ternary molecular interactions between transthyretin, A β peptides and small-molecule chaperones towards an alternative strategy for Alzheimer's disease drug discovery. *Journal of Medicinal Chemistry* **63**, 3205-3214.
- [48] Gamez J, Salvadó M, Reig N, Suñé P, Casanovas C, Rojas-Garcia R, Insa R (2019) Transthyretin stabilization activity of the catechol-O-methyltransferase inhibitor tolcapone (SOM0226) in hereditary ATTR amyloidosis patients and asymptomatic carriers: proof-of-concept study#. *Amyloid* **26**, 74-84.
- [49] Pinheiro F, Varejão N, Esperante S, Santos J, Velázquez-Campoy A, Reverter D, Pallarès I, Ventura S Tolcapone, a potent aggregation inhibitor for the treatment of familial leptomeningeal amyloidosis. *The FEBS Journal* **n/a**.
- [50] Sabri O, Seibyl J, Rowe C, Barthel H (2015) Beta-amyloid imaging with florbetaben. *Clinical and Translational Imaging* **3**, 13-26.
- [51] Son HJ, Jeong YJ, Yoon HJ, Lee SY, Choi GE, Park JA, Kim MH, Lee KC, Lee YJ, Kim MK, Cho K, Kang DY (2018) Assessment of brain beta-amyloid deposition in transgenic mouse models of Alzheimer's disease with PET imaging agents 18 F-flutemetamol and 18 F-florbetaben. *BMC Neuroscience* **19**.

- [52] Stenzel J, Rühlmann C, Lindner T, Polei S, Teipel S, Kurth J, Rominger A, Krause BJ, Vollmar B, Kuhla A (2019) [18F]-florbetaben pet/ct imaging in the alzheimer's disease mouse model APPswe/PS1de9. *Current Alzheimer Research* **16**, 49-55.
- [53] Waldron AM, Verhaeghe J, wyffels L, Schmidt M, Langlois X, Van Der Linden A, Stroobants S, Staelens S (2015) Preclinical Comparison of the Amyloid- β Radioligands [¹¹C]Pittsburgh compound B and [¹⁸F]florbetaben in Aged APPPS1-21 and BRI1-42 Mouse Models of Cerebral Amyloidosis. *Molecular Imaging and Biology* **17**, 688-696.
- [54] Brendel M, Jaworska A, Griebinger E, Rötzer C, Burgold S, Gildehaus FJ, Carlsen J, Cumming P, Baumann K, Haass C, Steiner H, Bartenstein P, Herms J, Rominger A (2015) Cross-sectional comparison of small animal [¹⁸F]-florbetaben amyloid-PET between transgenic AD mouse models. *PLoS ONE* **10**.
- [55] Rominger A, Brendel M, Burgold S, Keppler K, Baumann K, Xiong G, Mille E, Gildehaus FJ, Carlsen J, Schlichtiger J, Niedermoser S, Wängler B, Cumming P, Steiner H, Herms J, Haass C, Bartenstein P (2013) Longitudinal assessment of cerebral β -amyloid deposition in mice overexpressing swedish mutant β -Amyloid precursor protein using 18F-florbetaben PET. *J Nucl Med* **54**, 1127-1134.
- [56] Sacher C, Blume T, Beyer L, Peters F, Eckenweber F, Sgobio C, Deussing M, Albert NL, Unterrainer M, Lindner S, Gildehaus FJ, Von Ungern-Sternberg B, Brzak I, Neumann U, Saito T, Saido TC, Bartenstein P, Rominger A, Herms J, Brendel M (2019) Longitudinal PET monitoring of amyloidosis and microglial activation in a second-generation amyloid-b mouse model. *J Nucl Med* **60**, 1787-1793.
- [57] Zhang W, Oya S, Kung MP, Hou C, Maier DL, Kung HF (2005) F-18 Polyethyleneglycol stilbenes as PET imaging agents targeting A β aggregates in the brain. *Nucl Med Biol* **32**, 799-809.

- [58] Borchelt DR, Ratovitski T, Van Lare J, Lee MK, Gonzales V, Jenkins NA, Copeland NG, Price DL, Sisodia SS (1997) Accelerated amyloid deposition in the brains of transgenic mice coexpressing mutant presenilin 1 and amyloid precursor proteins. *Neuron* **19**, 939-945.
- [59] Episkopou V, Maeda S, Nishiguchi S, Shimada K, Gaitanaris GA, Gottesman ME, Robertson EJ (1993) Disruption of the transthyretin gene results in mice with depressed levels of plasma retinol and thyroid hormone. *Proc Natl Acad Sci U S A* **90**, 2375-2379.
- [60] Oliveira SM, Ribeiro CA, Cardoso I, Saraiva MJ (2011) Gender-dependent transthyretin modulation of brain amyloid- β Levels: Evidence from a mouse model of alzheimer's disease. *Journal of Alzheimer's Disease* **27**, 429-439.
- [61] Se HC, Leight SN, Lee VMY, Li T, Wong PC, Johnson JA, Saraiva MJ, Sisodia SS (2007) Accelerated A β deposition in APPswe/PS1 Δ E9 mice with hemizygous deletions of TTR (transthyretin). *Journal of Neuroscience* **27**, 7006-7010.
- [62] Li X, Zhang X, Ladiwala ARA, Du D, Yadav JK, Tessier PM, Wright PE, Kelly JW, Buxbaum JN (2013) Mechanisms of transthyretin inhibition of β -amyloid aggregation in vitro. *Journal of Neuroscience* **33**, 19423-19433.
- [63] Cascella R, Conti S, Mannini B, Li X, Buxbaum JN, Tiribilli B, Chiti F, Cecchi C (2013) Transthyretin suppresses the toxicity of oligomers formed by misfolded proteins in vitro. *Biochimica et Biophysica Acta - Molecular Basis of Disease* **1832**, 2302-2314.
- [64] Reixach N, Foss TR, Santelli E, Pascual J, Kelly JW, Buxbaum JN (2008) Human-Murine Transthyretin Heterotetramers Are Kinetically Stable and Non-amyloidogenic: A Lesson in the generation of transgenic models of diseases involving oligomeric proteins. *Journal of Biological Chemistry* **283**, 2098-2107.

- [65] Russ H, Müller T, Woitalla D, Rahbar A, Hahn J, Kuhn W (1999) Detection of tolcapone in the cerebrospinal fluid of parkinsonian subjects. *Naunyn-Schmiedeberg's Archives of Pharmacology* **360**, 719-720.
- [66] Codita A, Gumucio A, Lannfelt L, Gellerfors P, Winblad B, Mohammed AH, Nilsson LNG (2010) Impaired behavior of female tg-ArcSwe APP mice in the IntelliCage: A longitudinal study. *Behavioural Brain Research* **215**, 83-94.
- [67] Li X, Masliah E, Reixach N, Buxbaum JN (2011) Neuronal production of transthyretin in human and murine alzheimer's disease: Is it protective? *Journal of Neuroscience* **31**, 12483-12490.
- [68] Di Giovanni S, Eleuteri S, Paleologou KE, Yin G, Zweckstetter M, Carrupt PA, Lashuel HA (2010) Entacapone and tolcapone, two catechol O-methyltransferase inhibitors, block fibril formation of α -synuclein and β -amyloid and protect against amyloid-induced toxicity. *Journal of Biological Chemistry* **285**, 14941-14954.
- [69] Turner PV, Brabb T, Pekow C, Vasbinder MA (2011) Administration of substances to laboratory animals: Routes of administration and factors to consider. *Journal of the American Association for Laboratory Animal Science* **50**, 600-613.
- [70] Lewis RE, Kunz AL, Bell RE (1966) Error of intraperitoneal injections in rats. *Lab Anim Care* **16**, 505-509.